DOI: 10.13009/EUCASS2017-262

Aero-Thermal Post Flight Analysis of IXV Control Surfaces

Mario De Stefano Fumo, Roberto Scigliano*, Marika Belardo*, Giuseppe Rufolo*,*
*Angelo Esposito**, Mauro Linari***

** Italian Aerospace Research Centre (CIRA)*
Via Maiorise snc, 81043 Capua, Italy
*** MSC Software Srl*
Corso d'Italia 45, 00198 Roma, Italy.

Abstract

Hot structures made of Ceramic Matrix Composites (CMC) for space re-entry vehicles play a key role regarding the feasibility of advanced and reusable space transportation systems. In particular, looking to IXV experience and SPACE RIDER requirements, the need of a hot primary structure for the control surfaces is mandatory. In this framework, the validation with in-flight data of numerical tools capable to predict thermal and mechanical behaviour of a CMC component is of outmost importance. Scope of the paper is to present a finite element model for thermal and thermo-mechanical analyses of TPS components and its validation with IXV temperature data measured during the successful flight of 11 February 2015.

1. Introduction

CIRA has recently set up a research and development project with Italian industrial partners, with the aim at developing hot structures based on ceramic matrix composites technology. The project focuses on the application of this technology on a re-entry vehicle control surface. Besides the manufacturing process development, it is of paramount importance to have robust and reliable thermo-mechanical models for design, in which both the material anisotropy and the most representative heat transfer phenomena are modelled and validated.
The validation of numerical models is of outmost importance for the design of a re-entry vehicle. In particular, for what concern thermal protection system and hot structures design the definition of the right aerothermodynamic inputs and a faithful thermal and thermo-mechanical models are mandatory. Validation of aerothermodynamic and thermomechanical tools with respect to re-entry system flight data is a rare event.
With this respect, the Intermediate eXperimental Vehicle (IXV) flight offers a unique opportunity to validate and possibly improve the capability of the prediction tools with the perspective of reducing uncertainties significantly in favour of higher design robustness, reduced mass and eventually reduced development costs.
During the successful flight of 11th February 2015, about 300 sensors recorded the evolution of the most significant parameters while the spacecraft was crossing the harsh re-entry environment. In particular, with reference to Aerothermodynamics experiments, 194 thermocouples monitored the temperature of the various TPS components (both ceramic and ablative), and of the Cold Structure while 39 Kulite® sensors were used to measure pressure in various points of the vehicle surface.
The present work deals with the preliminary comparison between the in flight measurements and the predictions of an ad hoc developed thermo-mechanical model of the IXV body flap exploiting the Aerothermodynamic Database Tool (ATDB) developed by CIRA in the frame of the technical assistance provided to the European Space Agency through the Italian Space Agency as aerothermal input.

2. IXV Mission and Flight Data

The IXV mission was successfully performed on the 11th of February 2015 with 100% of the mission, system and technologies objectives successfully achieved [1].

DOI: 10.13009/EUCASS2017-262

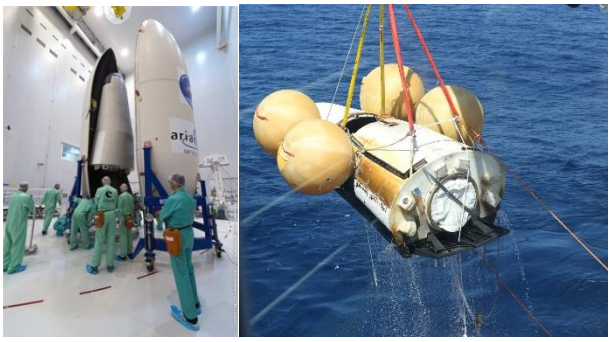

Figure 1. IXV during integration on VEGA and during recovery phase in Pacific Ocean after flight

The IXV system, and all associated technologies, have successfully performed the whole flight program in line with the commanded manoeuvres and trajectory predictions, performing an overall flight of approximately 25.000 km including 8.000 km in hot atmospheric re-entry environment with automatic guidance, starting from an orbital velocity of ~7.5 km/sec (Mach=27), concluding with precision splashdown in the Pacific ocean.
Data from all the sensors, in addition to trajectories data have been recovered both from flight telemetry and on board recorders [2].
The flown trajectory is shown in Fig. 2. It is quite close to the pre-flight prediction as well as to the nominal trajectory taken into account in the design phase, and is quite less demanding than the Maximum Heat flux dispersed trajectory used for the TPS design.

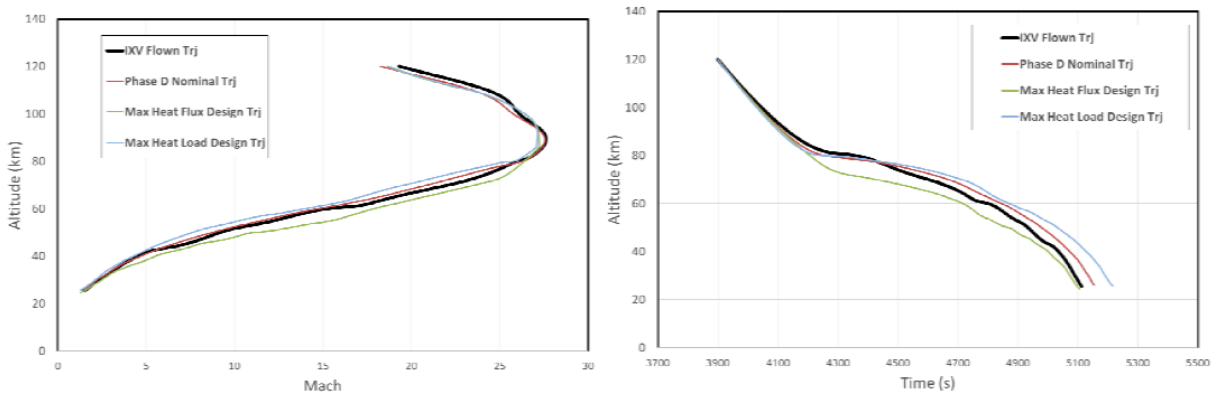

Figure 2. Flight Trajectory vs Design Trajectories

Flight altitude is derived from inertial measurement while the freestream conditions are obtained by applying an atmospheric model.
The data taken into account for the present preliminary analysis, in addition to the rebuilt trajectory, are temperatures measured during the flight by the thermocouples on the flaps as shown in Fig. 3. MT Aerospace provided the IXV Body Flaps with their patented technology Keraman® (C/SiC).

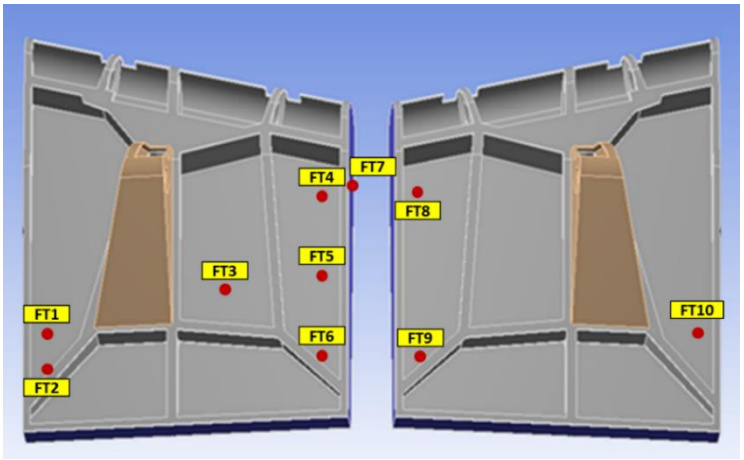

Figure 3. IXV Body Flaps Thermocouples Positions

DOI: 10.13009/EUCASS2017-262

3. Aerothermodynamic Tool and Loads

First step in the set-up of the validation process is the proper definition of the aerothermodynamics inputs to be used as boundary conditions for the thermo-mechanical simulation tool. Namely, convective heat flux as function of space and time has to be provided to the thermal analysts:

$$q_{conv} = q_{conv}(\bar{x}, t) \tag{1}$$

For each geometrical point of the body flap surface, the convective heat flux evolution along the flight trajectory is mainly driven by the following parameter:

- Trajectory asymptotic parameter, i.e. Mach, Temperature, density, driving the physics of the aerothermodynamics phenomena occurring during re-entry
- Vehicle attitude in terms of Angle of Attack and Angle of Sideslip, driving the bow shock shape, the evolution of the boundary layer through the vehicle windward and possible flow asymmetry
- Actual flaps deflection along the trajectory, driving the local flow phenomena acting on the control surface.

Therefore, the convective heat flux can be written as following:

$$q_{conv} = f\left(M_\infty, T_\infty, \rho_{\infty,} \alpha, \beta, \delta_{elevon}, t, \bar{x}\right) \tag{2}$$

with $\bar{x}$ varying over the flap surface.
In order to simplify the problem, a decoupling between time and spatial variation is applied by approximating the heat flux expression as following:

$$q_{conv} \approx f'\left(M_\infty, T_\infty, \rho_{\infty,} \alpha, \beta, \delta_{elevon}, t\right)_{x_{fixed}} \cdot f''(\bar{x})_{t_{fixed}} \tag{3}$$

where, f'corresponds to the time evolution along the trajectory of the heat flux on a prescribed point of the flap surface and f'' corresponds to a normalized heat flux distribution obtained at a certain instant of the flight trajectory.
The main assumption behind the validity of the above equation is that the flap deflection does not vary too much along the re-entry path. Indeed this was the case for the IXV trajectory as it is depicted in Fig. 4. All along the hypersonic flight regime the flap deflection remains quite limited and far enough from values capable of triggering shock wave boundary layer interaction phenomena that could significantly alter the space distribution.

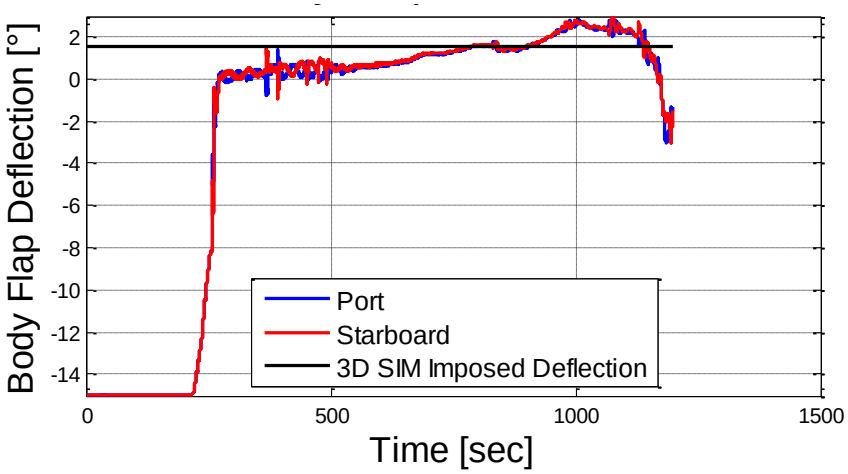

Figure 4. IXV Body Flaps Deflections during Flight and considered fixed deflection for PFA

A CFD computation performed by CIRA in the frame of IXV post flight analysis activities [3] at M=17.7, AoA=45deg and de=1.55deg in fully catalytic condition has been used to derive the heat flux spatial distribution kept constant along the trajectory. In Fig. 5 iso-contour of pressure and temperature for the above-mentioned computation are reported.

DOI: 10.13009/EUCASS2017-262

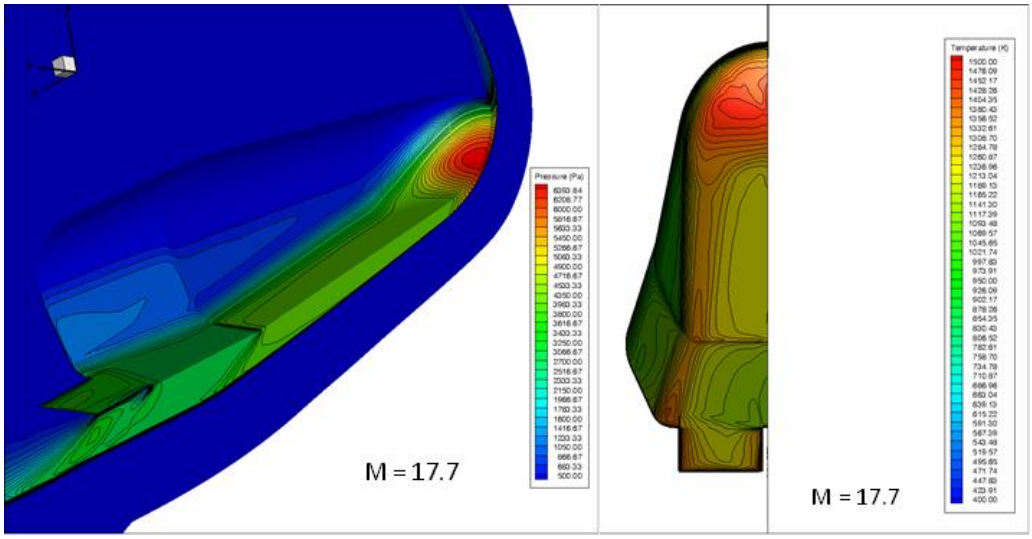

Figure 5. CFD computation used to derive heat flux distribution on body flap [3]

Time evolution of heat flux along the IXV flown trajectory for prescribed point of the body flap surface have been derived by applying the CIRA ATDB tool developed in the frame of the technical assistance provided to ESA within the IXV project [4].

CIRA ATDB is a numerical tool made up of different modules and capable of deriving the time history of heat flux, pressure and shear stress for a generic point of the IXV surface and for a generic re-entry trajectory. In synthesis the numerical tool combines the results of more than 200 CFD computations, suitably interpolated on a reference grid, taking into account the effects of Mach, angle of attack, angle of sideslip, flaps deflection. The CFD results are all expressed in terms of a non-dimensional parameter related with Stanton number so that they can be customized with respect to a generic flight trajectory. The ATDB tool also embeds a module for the prediction of two different types of laminar to turbulent transition: the one induced by the discrete step between the nose and the first row of shingle on the windward; the natural one occurring when the flap deflection is higher than a certain value, dependent from the asymptotic Reynolds and Mach number.

For the present activity, the ATDB tool has been used to generate the time history of heat flux along the IXV flown trajectory for both the control point F3 (this control point is on the windward, close to TC6), used for deriving the input to the 3D analysis, and the set of points corresponding to the thermocouples location, used for the 1D analysis. Results are reported in Fig. 6.

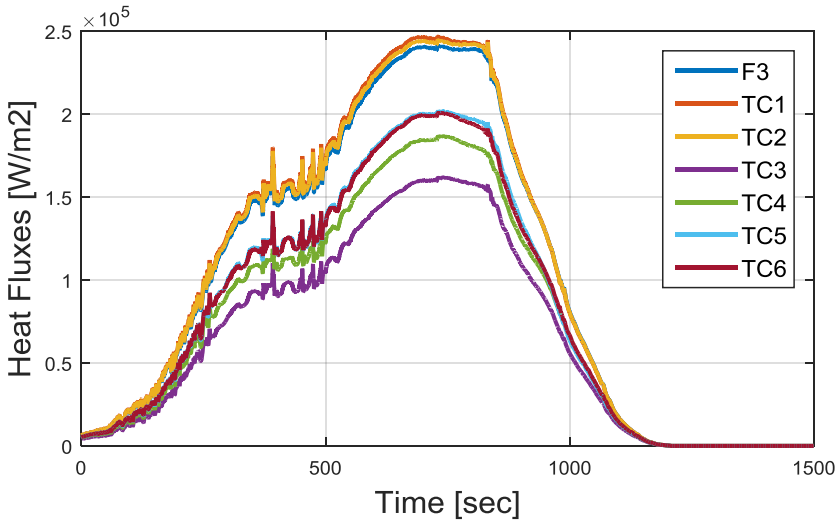

Figure 6. Heat flux input for fully catalytic and laminar case from ATDB tool.

DOI: 10.13009/EUCASS2017-262

4. Thermal Modelling Set-up

4.1 1D model

For a very preliminary assessment a 1-D thermal analysis have been performed on the geometric points where are located the thermocouples. Clearly, these calculations neglect: any in-plane conduction, taking into account only the conduction through the thickness; the face to face radiation in the flap backward. All the simplifications done with 1-D approach will be deeply investigated with the 3D FEM analysis presented in the next section. In order to reduce the effect of the neglected phenomena, the position of thermocouple TC3 has been considered. Indeed, TC3 is located in the centre of the flap, not too close to flap stringers, corners or edges. This approach leads to a preliminary analysis to check the boundary conditions to apply to full 3D model. Aero-heating inputs are taken directly from ATDB tool, as described in the previous section and take into account the real deflection of starboard flap.

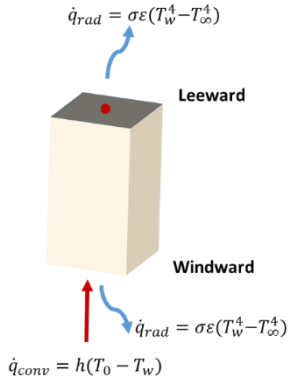

Figure 7. 1D CMC Body Flap Model and Boundary Conditions

A control volume analysis is used preliminary in the present work to derive a finite volume approach to the 1-D unsteady thermal analysis of CMC body flap. A finite volume approach is an intuitive technique that can be associated with the control volume analysis, that can be used to derive the heat diffusion equation. In the case of a one-dimensional control volume, the volume reduces to a length Δx, and the surface area reduces to unity; therefore, the energy conservation balance can be written as:

$$\left(\rho c_p \frac{\partial T}{\partial t}\right)\Delta x = \left(F_{cond_{in}} - F_{cond_{out}}\right) + \left(F_{conv_{in}} - F_{conv_{out}}\right) + \left(F_{rad_{in}} - F_{rad_{out}}\right) + Q_g \Delta x \qquad (4)$$

where the subscripts in and out refer respectively to the conductive, convective, and radiative heat fluxes into and out of the control volume in the x-direction. In the present model, no heat generation is considered (i.e. $Q_g = 0$). For each computational cells, conduction is taken into account. Convective heating ($F_{conv_{in}}$) is considered only for the first cell corresponding to flap windward, in the last corresponding to flap leeward it is neglected because it has been estimated three order of magnitude lower than windward. Convection cooling has been neglected ($F_{conv_{out}} = 0$). Radiation cooling ($F_{rad_{in}} = 0$) is considered on both windward and leeward faces.
From a numerical point of view, this is equivalent to a cell centered finite volume approach. The time derivative is approximate numerically using a first order backward difference; the conductive heat fluxes at cell interfaces are constructed numerically based on temperature in the cells on each side of the interface. The explicit integration scheme is applied as a simple function of temperature at the previous step, but the Fourier number must be less than or equal to 0.5 (for 1-D analysis) to maintain numerical stability [5]. In the present case, properties of Body Flap material, shown in Table 1, are taken from [6].

Table 1: Keraman C/SiC Thermal Properties [6]

	Temperature Range	**Values**
Density, kg/m3	RT	1800-2300
Thermal Conductivity, W/m K	RT	∥ 17 ⊥ 8
Specific Heat J/kg K	RT 1900 K	600 1600

DOI: 10.13009/EUCASS2017-262

Figure 8 shows the results of numerical computation for the geometrical control point FT3 where a thermocouple is located, for non-catalytic case. In the graph, it is evident how the radiative equilibrium hypothesis is not appropriate in case of relatively thin hot structure with relatively high thermal diffusivity, while when considering two surface emitting towards environment, is much more appropriate obtaining a temperature in its maximum value that is in the middle between windward and leeward maximum temperature during re-entry.

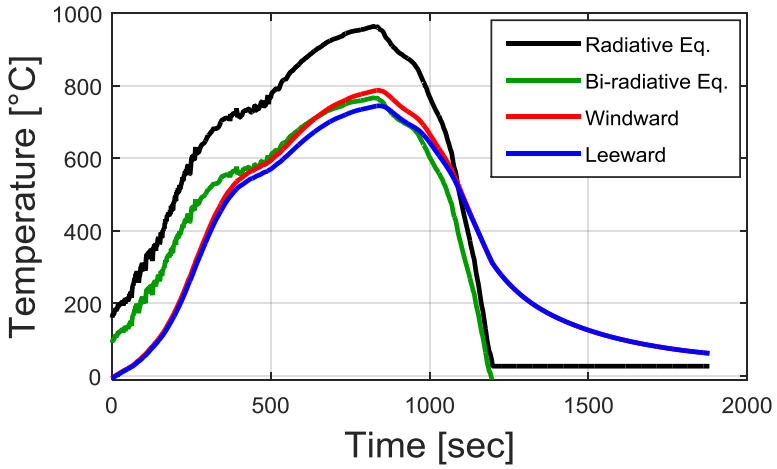

Figure 8. Numerical results of TC3 location for non catalytic laminar case

4.2 3D FEM model

In order to take into account the time variability of the re-entry phase, the modelling activity is usually aimed at carrying out a transient thermal analysis, followed by static structural analyses under thermo-mechanical loads [7].
The static structural analyses are carried out in the most critical instants (from a thermal point of view). Figure 9 shows the flow diagram of the analysis. The work presented in the paper focuses on the thermal analysis

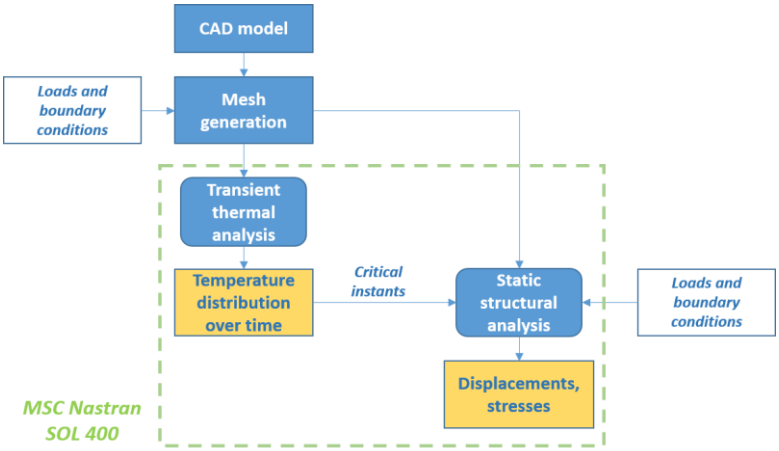

Figure 9. Flow diagram of analysis loop

The meshing and the post processing of data have been executed in MSC Apex and Patran environment. The solver is MSC Nastran, with activation of advanced nonlinear solution Sol 400.
The test case model is the IXV CMC flap. The analysis takes into account the following heat transfer phenomena (Fig. 10):

- Internal conduction
- Convection (heat flux typical of the re-entry of a reference spacecraft) on the lower surface of the model
- Radiation to ambient and between the facing surfaces (radiation enclosures)

DOI: 10.13009/EUCASS2017-262

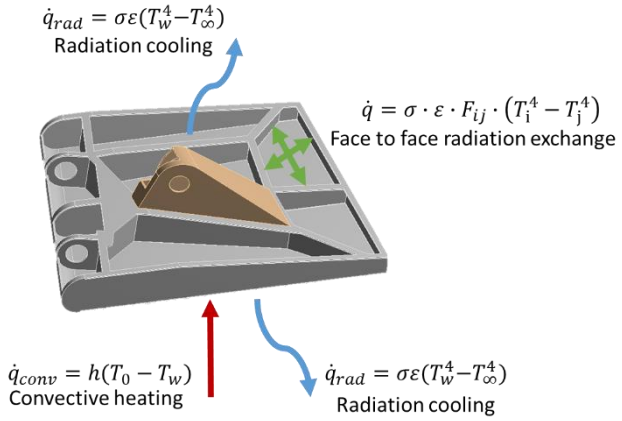

Figure 10. Main heat transfer phenomena considered in the model

The general thermal transient nonlinear problem (matrix form), which is solved in MSC Nastran, is the following:

$$[B]\{\dot{T}\} + [K]\{T\} + [R]\{T + T_{abs}\}^4 = \{P\} + \{N\} \tag{5}$$

where:

$[B]$	heat capacity matrix
$[K]$	heat conduction matrix
$[R]$	radiation exchange matrix
$\{P\}$	vector of applied heat loads that are constant or functions of time, but not functions of temperature
$\{N\}$	vector of nonlinear heat loads that depend on temperature
$\{T\}$	vector of grid point temperature
$\{\dot{T}\} = \left\{\frac{dT}{dt}\right\}$	Temperature time derivative
$\{T_{abs}\}$	the absolute temperature scale adjustment required for radiation heat transfer exchange or radiation

Eq. 5 is solved by using a Newton-Raphson iteration scheme.
As regards the thermal properties, the material has been modelled as orthotropic.
Radiation and convection are treated as boundary conditions.
For the present test case the convective heat flux has been modelled by means of the following "free convection" formulation:

$$\dot{q} = H \cdot u_{CNTRLND} \cdot (T - T_{amb}) \tag{6}$$

Where the time-variability of convective heat transfer coefficient H is introduced by means of the time-dependent function $u_{CNTRLND}$, which has a formulation of the type:

$$\{u_{CNTRLND}(t)\} = \{A\} \cdot F(t - \tau) \tag{7}$$

Where $\{A\}$ is a time-independent vector of amplitudes and $F(t - \tau)$ is a function of time.
The radiation exchange of the model to free space is implemented by the formula:

$$\dot{q} = \sigma \cdot \varepsilon \cdot \left(T_{surf}^4 - T_{amb}^4\right) \tag{8}$$

where:

σ	Stefan-Boltzmann constant (5.67E-8 W/m^{2}K^4)
T_{surf}	surface temperature
ε	emissivity
T_{surf}	radiation sink temperature

DOI: 10.13009/EUCASS2017-262

The radiation exchange between two grey bodies depends on the geometric view factor F_{ij}:

$$\dot{q} = \sigma \cdot \varepsilon \cdot F_G \cdot (T_1^4 - T_2^4)_{ij} = \sigma \varepsilon F_{ij} (T_i^4 - T_j^4) \quad (9)$$

Initial temperature of the flap has been set at 273 K while ambient temperature follows the real values coming from the re-entry mission profile.

The FE model for thermal and thermo-mechanical analysis (MSC Nastran SOL 400) is made up of about 73710 nodes and 44000 3D HEXA elements and few WEDGES and TETRA 3D elements. Figure 11 shows the geometry of the model.

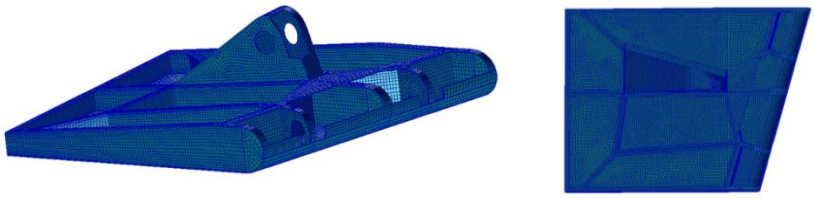

Figure 11. Geometry

5. Results

5.1. Numerical/Experimental Correlation

A first comparison has been performed on the position of thermocouples FT3, located in the central area of the leeward of the left flap. Figure 12 shows the numerical results obtained by means of 1D simplified model with fully catalytic and non-catalytic assumptions, with the laminar-turbulent transition as predicted by ATDB tool and without transition. Some considerations on 1-D results:
1. Experimental curve lies on non-catalytic simulations;
2. The laminar-turbulent transition foreseen by ATDB tool[1] and used for design was not detected during IXV flight;
3. Initial heating obtained by CFD computations with continuum regime assumption overestimates heat fluxes. In the first 400 s of the re-entry, the vehicle flew between 120 and 80 km from rarefied to transitional regime. It is a well-known phenomenon, but it was considered as a further conservativeness for TPS and HS design. In order to better re-build flight data dedicated transitional and rarefied computations would be needed.
4. The cooling phase is quicker in numerical modelling than in flight experience; considering the model the choice to neglect the convection heating on the leeward should be reconsidered in future simulations.

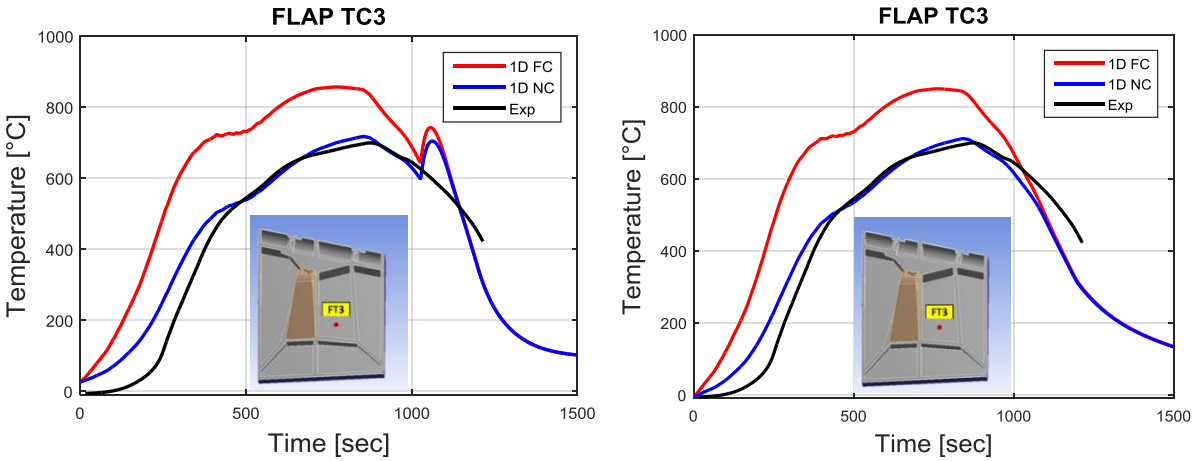

Figure 12. Numerical-experimental comparison for laminar turbulent transition imposed and laminar cases

Two different 3D runs respectively with non-catalytic and fully catalytic hypothesis have been performed with the full model as described in section 4.2. The Body Flap thermal evolution have been simulated for 1875s as the whole mission

[1] For design purposes a sizing step was imposed at nose/shingle junction. The actual step realised during IXV integration was much lower thus explaining the differences between ATDB predictions and flight.

DOI: 10.13009/EUCASS2017-262

timeline. In both the simulations, normalized heat fluxes follow the same CFD spatial distribution as reported in section 3, but the heat fluxes history took into account surface catalysis conditions. Figure 13 and Figure 14 show the temperature map for the non-catalytic model and fully catalytic model at the time 826 s in which the overall max temperature is reached. It can be seen how the maximum temperature values are in the right bottom corner area. This is consistent with heat fluxes distribution. Maximum numerical temperature around 1135°C (1410 K) for the non-catalytic model and 1345°C (1620 K) for the full catalytic.

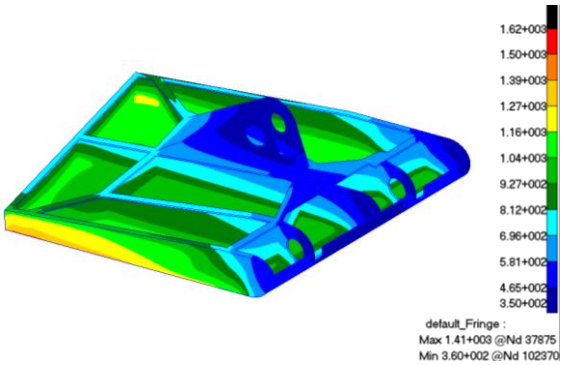

isometric view

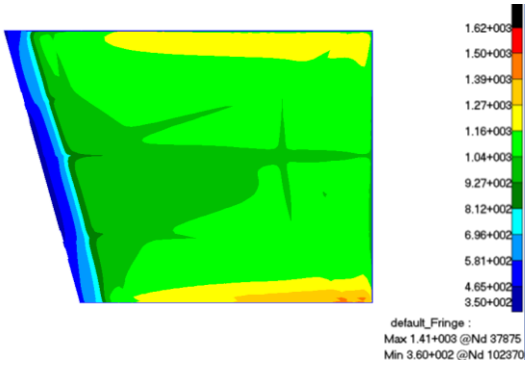

bottom view

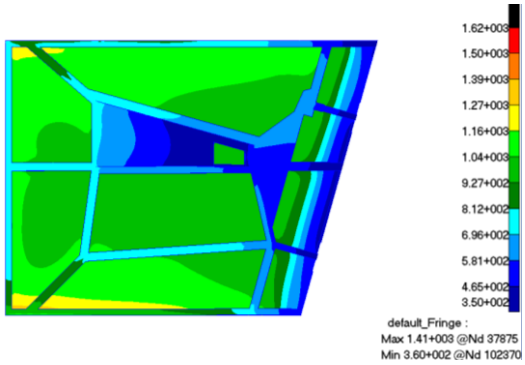

top view

Figure 13. Non catalytic heat fluxes. Temperature distribution at max temperature peak i.e. time =826s

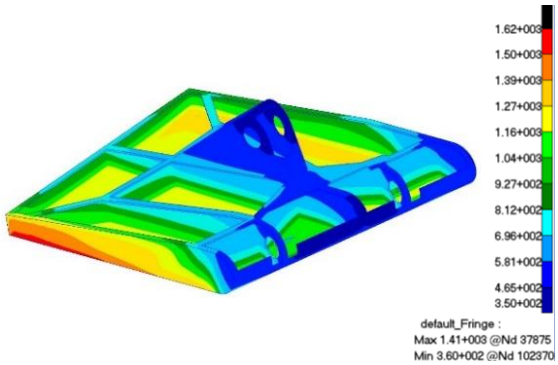

isometric view

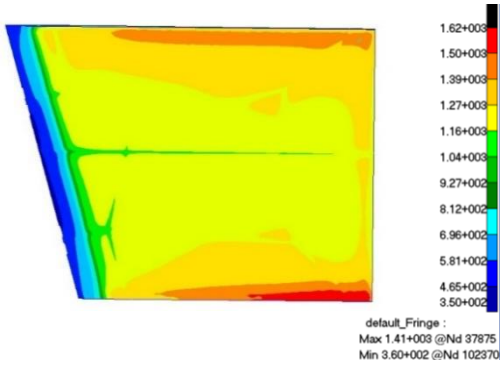

bottom view

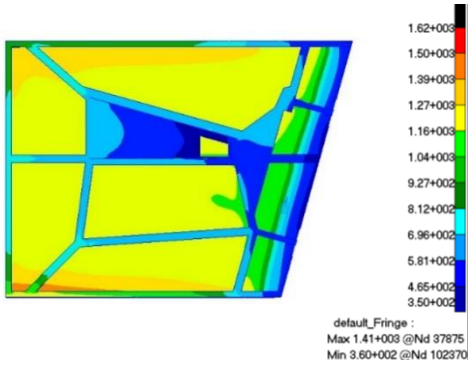

top view

Figure 14. Fully catalytic heat fluxes. Temperature distribution at max temperature peak i.e. time =826s

Figure 15 shows the temperature on the interfaces with rod for the actuation (support) and with the attachments with cold structure (hinge) for the fully catalytic case. The maximum temperature achieved at the hinge attachments was certainly below 600° C obtained for fully catalytic computation.

Comparison between 1D and 3D models shown in figure 16 demonstrate a good agreement between non-catalytic numerical results and measured temperatures. Figure 2 shows also symmetrical points on right flap. All TC's show a regular temperature evolution and consistency between each other also considering the symmetric positions. Only TC4 shows higher temperature with respect to non-catalytic numerical results and with respect to symmetric TC8 measurement.

DOI: 10.13009/EUCASS2017-262

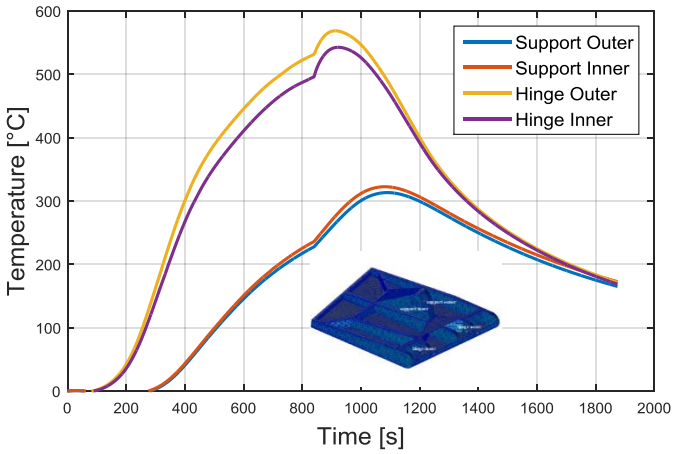

Figure 15. Temperature on interfaces between Body Flap and actuation rod and with attachments with cold structure.

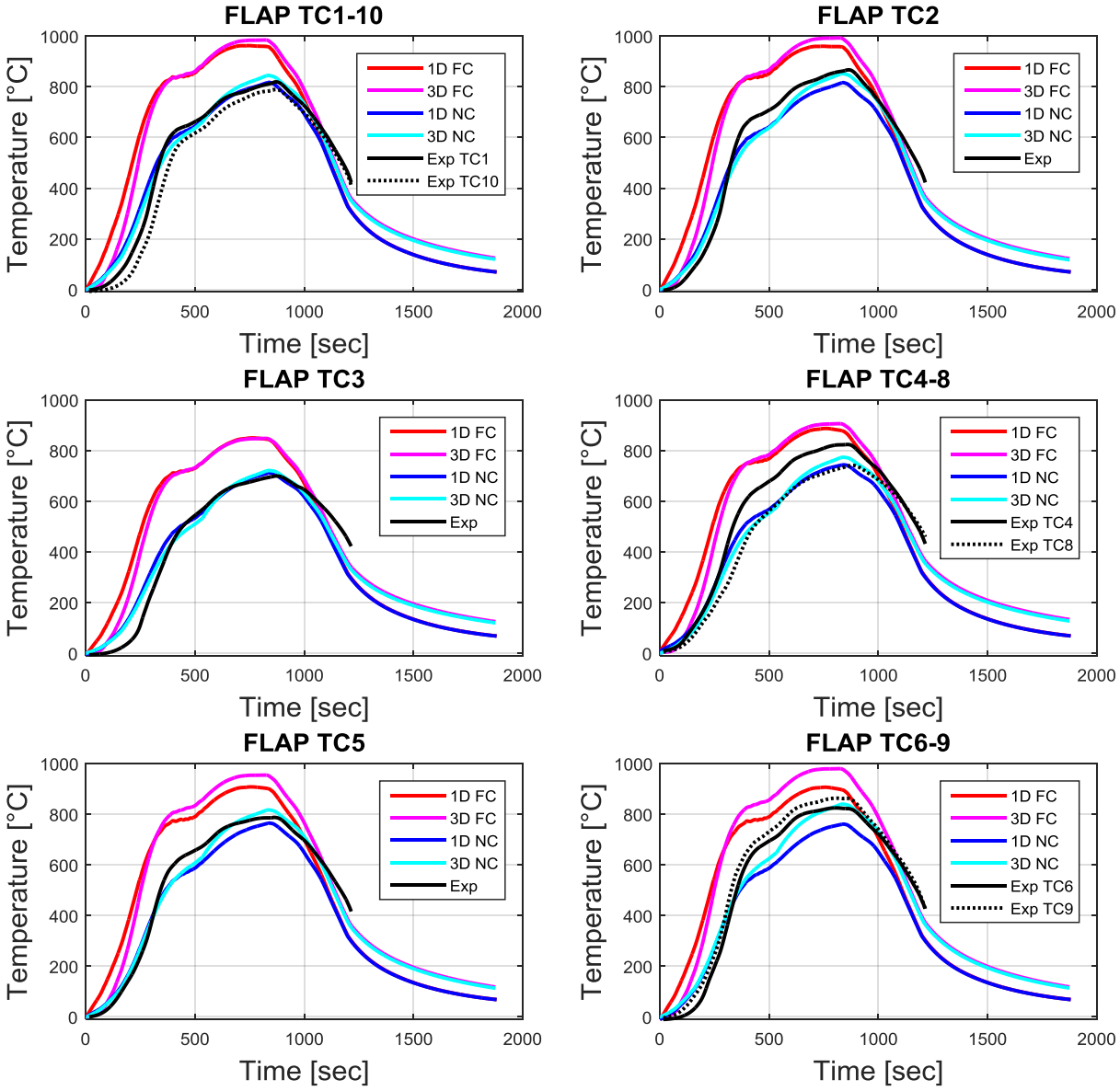

Figure 16. Numerical-experimental comparison for 1D and 3D models for laminar case

DOI: 10.13009/EUCASS2017-262

For what concern the 1D model, the experimental curves lie on non-catalytic simulations giving raise to the fact that the flap CMC material up to 1000°C has a very low catalytic behavior. Furthermore, the 3D model, underestimates the cooling phase temperature. A detailed analysis using aerothermal distribution also on flap leeward has to be performed in order to get better predictions.

6. Conclusions

A thermo-structural model of the IXV Body Flap has been developed in MSC Nastran with the aim to validate it with flight data coming from IXV flight. The developed methodology will be applied for future activities on analysis and design of CMC thermal protection system and hot structure of re-entry and hypersonic vehicle. In addition, a simplified 1D model has been developed for preliminary assessment.
The analysis has been focused on the temperatures measured by ten thermocouples placed on the leeward side of C/SiC Body Flaps. The following conclusions can be drawn:

- Flight temperatures are well correlated with non catalytic results, showing that a fully catalytic approach risks to be very conservative for design purpose;
- The initial temperature ramps are not reproduced correctly, due to the aero-heating loads obtained without considering rarefaction effect, that are very important in the first 400 s when the vehicle flies above 80 km.
- Some discrepancies occur in the cooling phase, probably due to the simplified model assumption that does not take into account heating on the flaps leeward. These heat fluxes could not be neglected when windward heating reduces and radiation cooling starts to be effective.

The IXV post flight analysis is still ongoing; future activities will be focused on detailed investigation of phenomena not accounted for in the present analysis: e.g. rarefied effects, convective heating on leeward side.

Acknowledgements

The authors wish to thanks the European Space Agency, the Italian Space Agency and the IXV Prime Contractor Thales Alenia Space Italia for giving the opportunity of exploiting such unique and valuable set of flight data.
Present activity has been funded by the Italian Aerospace Research Program (PRO.R.A.).

References

[1] G. Tumino et al., "The IXV Programme from Design to Flight Experience", IAC-15-D2.6, *66th IAC, Gerusalem*, October 2015.
[2] Rufolo, G.C., Camarri, F., Pereira C., Romani, R., Vernani, D., "ESA Intermediate Experimental Vehicle In-Flight Experimentation. Objectivies, Experiment Implementation, Qualification and Integration," IAC-14-D2.6.3, 65th, International Astronautical Congress, Toronto, Canada, 2014.
[3] P. Roncioni, G. Ranuzzi, G. Rufolo, A. Schettino, M. De Stefano Fumo, Preliminary Numerical Rebuilding of IXV Flight Aeroheating, 8th Thermal Protection System and Hot Structure Workshop, ESA ESTEC, Noordwijk, 19-22 April 2016.
[4] Di Benedetto, S., Rufolo G.C., Marini M., European Space Agency Intermediate eXperimental Vehicle: Development of an Independent Aerothermodynamic Database Tool, Journal of Aerospace Engineering, February 1, 2013. DOI: 10.1177/0954410012469493.
[5] Incropera, F.P., and De witt, D.P., Introduction to Heat Transfer, 3rd Ed., John Wiley & Sons, Inc.,1996.
[6] Handrick, K. E., Ceramic Matrix Composites (CMC) for demanding Aerospace and Terrestrial Applications. In: XXI Congress AIV, 2013.
[7] R. Scigliano, M. Belardo, M. De Stefano Fumo, A. Esposito, Thermo-Mechanical Numerical Model Set-up and Validation Approach for a CMC Control Surface for Re-entry Vehicles, SPACE Conference and Exposition, AIAA SPACE 2016, 13-16 September 2016, Long Beach, California, USA, DOI: 10.2514/6.2016-5626.